



Synergistic effects of conductive PVA/PEDOT electrospun scaffolds and electrical stimulation for more effective neural tissue engineering

Ali Babaie^{a,b,1}, Behnaz Bakhshandeh^{c,*}, Ali Abedi^{a,1}, Javad Mohammadnejad^a, Iman Shabani^d, Abdolreza Ardeshtyrlajimi^e, Seyed Reza Moosavi^f, Javid Amini^g, Lobat Tayebi^{h,*}

^a Department of Life Science Engineering, Faculty of New Sciences and Technology, University of Tehran, Tehran, Iran

^b Department of Chemistry and Biotechnology, Faculty of Science Engineering and Technology, Swinburne University of Technology, Hawthorn, Victoria 3122, Australia

^c Department of Biotechnology, College of Science, University of Tehran, Tehran, Iran

^d Department of Biomedical Engineering, Amir Kabir University of Technology, Tehran, Iran

^e Department of Tissue Engineering and Applied Cell Sciences, School of Advanced Technologies in Medicine, Shahid Beheshti University of Medical Sciences, Tehran, Iran

^f Faculty of Pharmacy, Tehran University of Medical Sciences, Tehran, Iran

^g Department of Mechanical Engineering, Islamic Azad University, Science and Research Branch, Tehran, Iran

^h Marquette University, School of Dentistry, Milwaukee, WI 53201, USA

ARTICLE INFO

Keywords:

Polyvinyl Alcohol

PEDOT:PSS

Electrical Stimulation

Mesenchymal Stem Cells

Neural Tissue Engineering

ABSTRACT

Fabrication and optimization of conductive scaffolds capable of inducing proper intercellular connections through electrical signals is critical for neural tissue engineering. In this research, electrospun conductive PVA (Polyvinyl alcohol)/PEDOT(poly(3,4-ethylenedioxythiophene)) scaffolds were fabricated in different compositions. Conductivity of electrospinning solutions and electrospun scaffolds were measured. Morphology and topography, mechanical properties and water contact angle of scaffolds were analyzed. Chemistry of scaffolds were studied using FTIR analysis, while biocompatibility and cellular interactions with scaffolds were tested using MTT assay and cellular attachment and spreading testing. Our results show improvements in PEDOT-containing scaffolds, in terms of physiochemical properties, and cell viability compared to pure PVA scaffolds. After optimization of scaffolds, real-time PCR analysis was used to study neural differentiation of rat mesenchymal stem cells (MSCs). Scaffold samples with and without induction of electrical stimulation are shown to upregulate β -tubulin, nestin and enolase as compared to TCP samples. Additionally, expression of nestin gene in scaffold samples with electrical stimulation was 1.5 times more significant than scaffold sample. Overall, this study shows that using PVA/PEDOT conductive scaffolds with electrical stimulation can improve cellular response and neural differentiation through mimicking the properties of native neural tissue.

1. Introduction

Regeneration of peripheral nerve injuries occurs at a limited rate in body, therefore these injuries can cause permanent damage to patients. Current methods in treatment of these injuries are through autologous grafts. Application of autologous grafts are highly limited due to availability of donors and high expenses. Allografts and xenografts have been also used, but showed limited success due to issues including immune response and possible rejection of grafts [1-4]. Using *in vitro* methods combined with all the advances in micro-/nano-fabrication, tissue engineering is suggesting new solutions for engineering of neural tissue [5]. However, successful engineering of neural tissue depends on providing a balance between cellular behavior and growth of cells into

the synthetic scaffold.

In order to achieve functional differentiation of stem cells, properties of the scaffolds should mimic the biophysical cues of natural environment of the target tissue [6]. In order to mimic these cues, engineering of neural tissue should be performed on biocompatible, biodegradable conductive scaffolds [2,7-9]. Electrospinning is one of the most accepted methods in fabrication of neural tissue engineering scaffolds due to simplicity, low expenses and ease of control over morphology and structure of fibers [10-12]. Electrospun scaffolds have superior physical and chemical properties, which is suitable for various applications including nerve growth conduits, neural probes and neural tissue engineering scaffolds. Microfibrillar scaffolds are formed from fibers with diameters of a few microns down to few hundreds of

* Corresponding authors.

E-mail addresses: b.bakhshandeh@ut.ac.ir (B. Bakhshandeh), lobat.tayebi@marquette.edu (L. Tayebi).

¹ Authors have contributed equally in experimental work.

nanometers that can promote attachments and growth of cells [7,13,14].

As neural tissue is a stimuli-responsive tissue, fabrication of an electrically conductive scaffold—capable to transmitting electrical signals—can substantially improve differentiation of stem cells [5,15–17]. Previous researches have mainly focused on using carbon nanotubes (CNTs), Polypyrrole (PPy) and Polyaniline (PANI) for fabrication of conductive scaffolds [18]. Meanwhile, poly (3,4-ethylenedioxythiophene) (PEDOT) is a polythiophene derivative that has recently drawn a lot of attention in biomaterials and tissue engineering applications due to its biocompatibility and chemical stability. Also, as compared to PPy, PEDOT has higher electrical and thermal conductivity [7,18–20]. Currently, PEDOT is being used in fabrication of biosensors, neural electrodes and in environmental applications [18,21]. PEDOT showed biocompatibility in culture of different cell types, including mesenchymal stem cells (MSCs) extracted from rat bone marrow [7] and neural cells [22]. PEDOT substrates doped with either polystyrene sulfonate (PSS) or tosylate have supported attachment and growth of fibroblasts [23]. SH-SY5Y neuroblastoma cells showed suitable attachment and growth on PEDOT-coated PET substrates [24]. In this study, PVA is used as a carrier polymer for electrospinning. PVA is a synthetic polymer with high hydrophilicity (–OH groups) that has been widely used in tissue engineering due to its good biodegradability and excellent biocompatibility [25].

Electrical stimulation is another factor we have utilized in this study. Presence of electrical current can be very effective in mimicking the electrochemical cues surrounding nerve cells and differentiation of MSCs into the neural cell lines. Applying electrical charge affects the action potential of the cell membrane, changing the influx of calcium ions which can facilitate the differentiation process [18,26–28]. Also, electrical stimulation has a significant effect on intracellular signaling pathways and cells' intracellular microenvironment. Activation of these pathways facilitates migration, proliferation and differentiation of cultured cells [26,29].

Favorable properties of PEDOT in contact with neural tissue is established and supported with a huge amount of research. However, to best of our knowledge, no research has focused on fabricating and optimizing conductive composite scaffolds with PEDOT and PVA through electrospinning for mimicking the natural environment of neural tissue. Afterwards, we evaluate the differentiation of MSCs using these scaffolds and electrical stimulation.

2. Materials and methods

2.1. Materials

Dulbecco's Modified Eagle's Medium (DMEM), Trypsin/EDTA, Penicillin/Streptomycin, fetal bovine serum (FBS) and phosphate-buffered saline (PBS) were purchased from Gibco. MTT powder, Trypan Blue, PEDOT:PSS (483095) and PVA (99% hydrolyzed) were purchased from Sigma-Aldrich. DMSO, ethanol, glutaraldehyde and glycine were purchased from Merck.

2.2. Scaffold fabrication

In this research, six compositions of scaffolds are fabricated using PVA and PEDOT:PSS. PVA (12 wt%) was dissolved overnight in deionized water at 80 °C using a magnetic stirrer. Afterwards, the PVA solution was cooled down, combined with different amounts of PEDOT:PSS and mixed with magnetic stirrer for another 12 h to form homogenized aqueous dispersion for electrospinning.

Details of different electrospinning solutions are shown in Table 1. Conductivity of solutions were measured in room temperature using a conductometer (WPA-CMD510) prior to placing solutions into syringes for electrospinning. Measurements were carried out five times for each sample and conductivity values have been reported in the form of

Table 1

Details of content and electrical conductivity of electrospinning solutions.

Sample	PEDOT content (wt. %)	Electrical conductivity of electrospinning solution (μS/cm)
PVA	0	198 ± 7
PVA/ PEDOT(0.1)	0.1	491 ± 10
PVA/ PEDOT(0.3)	0.3	557 ± 11
PVA/ PEDOT(0.6)	0.6	731 ± 11
PVA/ PEDOT(1)	1	825 ± 14
PVA/ PEDOT(3)	3	1050 ± 12

average ± standard deviation (Table 1). After optimization of electrospinning parameters, including needle-to-drum distance, applied voltage and concentration of solution, samples were electrospun using a dual-nozzle setup (flow rate of 0.4 ml/h each) in an electrospinning device (Full Option Lab electrospinning device – Nanoazma - Iran) onto aluminum foils. All samples were fabricated using a 25 KV of voltage at the tip of the nozzle, with 18 cm needle-to-drum distance on the rotating drum (1000 rpm). After completion of electrospinning process, nanofibrous mats were removed from aluminum collector. Samples were cross-linked by exposure to glutaraldehyde vapor, which was placed at the bottom of the desiccator at 0.2 M concentration. In order to remove the excessive glutaraldehyde after crosslinking, scaffolds were washed with 1% wt/wt aqueous glycine for 15 min and rinsed extensively with PBS [7].

2.3. Scaffold characterization

Structural morphology of electrospun nanofibers were evaluated using a scanning electron microscope (Hitachi S-4160 and Seron Technologies AIS2100). Fiber diameter was measured using Image J (Image J - National Institutes of Health, USA), and statistical analysis was performed using Microsoft excel software. Surface topography was evaluated using Olympus OLS4100 digital laser scanning microscope pictures, and surface roughness was evaluated using OLS4100 offline V3.1.1 software (Olympus Corporation, Japan). Contact angle measurements were carried out using OCA 15EC (Dataphysics, Germany).

Water contact angle was measured by placing a 4 μl water drop on the surface of scaffolds at room temperature. Measurement was carried out for a minimum of eight times for each sample.

In order to confirm the expected bonds and functional groups, Fourier Transform Infrared Spectroscopy (FTIR) was performed. PEDOT:PSS solution was placed in a freeze-dryer overnight to obtain a dry PEDOT:PSS sample. Pure PVA powder and punched sample from PVA/PEDOT(1) scaffold was dried in vacuum oven at 30 °C overnight to remove any residual water content. Samples were recorded using FTIR spectrometer (PerkinElmer-Frontier L1280032) against a blank KBr pellet background.

Mechanical behavior of cross-linked scaffolds was evaluated using Instron 3367 tensile testing device (Instron co., UK). Scaffolds with dimensions of 5 × 30 mm (3 replicates each) were punched from a single cross-linked electrospun sheet. Samples were tested at room temperature with 1 mm/min loading velocity.

Electrical conductivity of cross-linked scaffolds has been measured using Keithley model 2361 multimeter (Keithley Instruments, USA). Three 10 × 1 mm samples were cut from each electrospun sheet, and the thickness of each sheet was measured. Resistance (R) of fibers was calculated by measuring current during applying a range of voltage from –10 V to 10 V with 0.2 V steps into samples using 1 mm electrodes. Electrical conductivity of fibers (σ) has been measured using Eq. (1) considering the size and thickness of samples.

$$\sigma = l / (w \cdot d \cdot R) \quad (1)$$

where *l* is distance between two electrodes, *w* is the width of electrode and *d* is thickness of scaffold sample.

2.4. Biocompatibility studies

To evaluate the biological behavior of the scaffold, crosslinked scaffolds have been punched to fit the bottom of 24-well plates, sterilized with 70% v/v aqueous ethanol solution, washed with PBS, incubated overnight in complete culture medium (DMEM high glucose, 10% FBS and 1% Penicillin/Streptomycin) and seeded with 2×10^4 of rat MSCs per well. Culture medium was changed once every 2 days. Adhesion and spreading of cells have been monitored after 1 and 7 days of culture. After the incubation period, cells were rinsed with PBS to remove dead and unattached cells, fixed with 2.5% aqueous glutaraldehyde solution for 3 h, and washed respectively with 60, 70, 80, 90 and 100% aqueous ethanol solution for 15 min to remove the residual water content. Images of surface were taken using Seron Technologies AIS2100 scanning electron microscope device.

To analyze the metabolic activity and proliferation rate of the seeded cells, scaffolds were punched, sterilized and incubated in complete culture medium. The cells were then seeded on scaffold samples together with tissue culture plates (TCP) and treated similar to adhesion section as mentioned above. The proliferation rate based on metabolic activity has been monitored after 1, 3 and 7 days of culture. After the incubation period, cells were rinsed with PBS solution, and incubated for 4 h with 0.5 mg/ml MTT solution. Lastly, the medium was removed, then the developed formazan crystal was dissolved with DMSO and pipetted out into 96-well plates. Absorbance was recorded at 540 nm. All samples were analyzed in triplicates and reported in terms of average optical density (O.D.) with standard deviation.

2.5. Neural differentiation studies

In order to evaluate the differentiation behavior of rat MSCs seeded on conductive scaffolds, cells were cultured on scaffolds and TCPs and treated with different inductions (see Table 2). Initially, cells were seeded at density of 1.5×10^5 cells/well of 6-well plates on different surfaces and incubated for 24 h prior to induction of differentiation. Afterwards, as shown in Fig. 1, Fig. 7 differentiation groups were treated with DMEM as basal medium, FBS and 2.5 μ M retinoic acid (RA), 0.5 mM Forskolin and 2.5 μ M 3-isobutyl-1-methylxanthine (IBMX) for 14 days; medium was changed every 2 days. The amount of FBS was reduced during the differentiation protocol to apply FBS shock, where 10v/v% was being applied in day 0 to day 4, 5v/v% was being applied in day 5 to day 10, and 2v/v% of FBS was being applied in day 11 to day 14. In treatment of Scaffold + ES group, electrical stimulation was applied during day 10 to day 13 using an electrical pulse generator (GPS-2105 function generator, General Polytronic). Electrical stimulation was applied using 100 mV/mm of scaffolds for 2 h each day. The bioreactor for electrical stimulation (Figure S1) included two 316-stainless steel electrodes for each well, where the electrodes were connected to pulse generator using copper wires.

After day 14 of differentiation, RNA was extracted from each sample, cDNA was synthesized, and expressions of neural marker genes—nestin, enolase and β -Tubulin III—were analyzed using qPCR. Primers used in qPCR are listed in Table S1, and HPRT was applied as the housekeeping gene.

Table 2
Different differentiation study groups and their treatments.

Samples	Scaffold	Differentiation media (DM)	Electrical stimulation (ES)	Named as
MSC on TCP	–	+	–	TCP + DM
MSC on scaffold	+	+	–	Scaffold + DM
MSC on scaffold	+	+	+	Scaffold + DM + ES
MSC on TCP	–	–	–	Control

3. Results and discussion

3.1. Morphological properties of the scaffolds

Scaffolds containing different amounts of PVA and PEDOT:PSS, as described in Table 1, were fabricated by electrospinning. Fig. 2 shows the microscopic structure of different scaffold samples, which demonstrates that all scaffolds are bead-free with uniform structures. Figure S2 illustrates the average diameter and fiber diameter distribution of each scaffold.

Increasing the amounts of low concentrated PEDOT:PSS (1.3 wt%) to pure PVA solution of 12% wt/wt concentration lead to a less concentrated solution. Moreover, as shown in Table 1, solution conductivity has risen meaningfully. Our results show that mean fiber diameter decreases significantly in all samples containing PEDOT compared to PVA samples, except for PVA/PEDOT(3). Also, a decreasing trend in average fiber diameter has been observed in samples (p value ≤ 0.05). The lowest average of fiber diameter among samples was 300 nm in PVA/PEDOT(3) samples, which shows a significant 40% decrease as compared to PVA samples with 500 nm of average fiber diameter. Moreover, the range of fiber diameters have changed from 450 to 700 nm in pure PVA samples to 200 to 400 nm in PVA/PEDOT(3). Fiber diameter distribution also illustrates a gradual decline pattern in mode value of fiber diameter from pure PVA (500 nm) to PVA/PEDOT(1) (350 nm).

According to previous investigations, lower concentration and higher conductivity of solutions will both lead to spinning of narrower fibers, which is in consent with our results [7,31–33]. Other studies on electrospinning of fibers showed that increase in concentration from 80 to 140 mg/ml results in increase of average diameter of fibers from 120 to 610 nm [32]. In other researches on conductive composite fibers, adding 1 wt% PEDOT to CS/PVA scaffolds have resulted in a 4-time increase in conductivity of solutions and 50% decrease in diameter of fibers [7].

3.2. Chemical properties of the scaffolds

In order to evaluate the functional groups present in different scaffolds, FTIR analysis was conducted, with the results shown in Fig. 3 and Figure S3. The large peaks at 3278 cm^{-1} in PVA sample and $\sim 3350 \text{ cm}^{-1}$ in PEDOT-containing scaffolds are related to the stretching of O–H bond [7,34]. Peak at 3125 cm^{-1} in PEDOT:PSS is related to stretching of C–H bond in aromatic ring of PSS [7]. This peak in PEDOT-containing scaffolds is overlapping with the large peak related to O–H stretching. Another peak at $\sim 2941 \text{ cm}^{-1}$ in PVA and PEDOT-containing scaffold samples is related to stretching of C–H in PVA [34]. The peaks at 1737 cm^{-1} in PVA scaffold and at $\sim 1733 \text{ cm}^{-1}$ in scaffold samples are related to stretching of C=O in acetaldehyde functional groups, which are formed during the uncatalyzed tautomeric reaction in vinyl alcohol monomers [7,34,35]. Peaks at 1719 cm^{-1} in PEDOT:PSS sample and in 1680 cm^{-1} in PEDOT-containing scaffolds are attributed to the stretching of C=C in thiophene ring [7,36]. Peaks at 1374 cm^{-1} and 1434 cm^{-1} in PEDOT-containing scaffolds, and at 1380 cm^{-1} and 1446 cm^{-1} in PVA sample, are related to the bending of C–H bond in PVA [7,34,37]. The peaks at 1450 cm^{-1} and 1510 cm^{-1} in PEDOT:PSS sample and in scaffold samples are related to

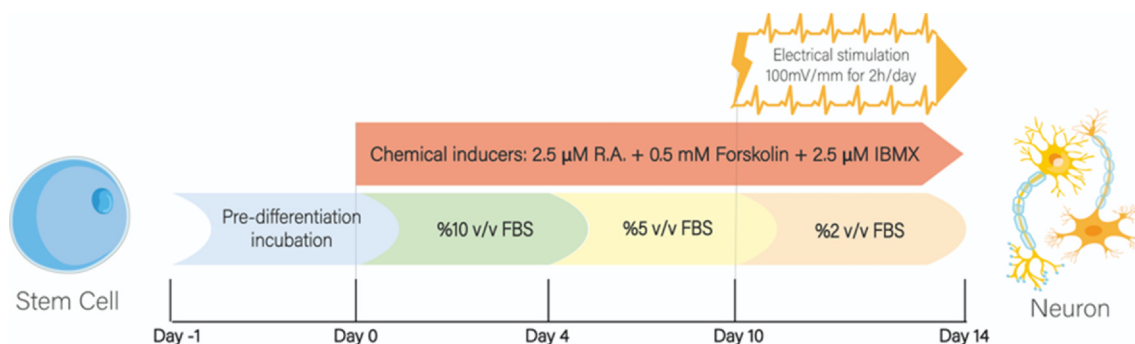


Fig. 1. Infographic illustration of the applied differentiation protocol for differentiation of MSCs into neuron-like cells.

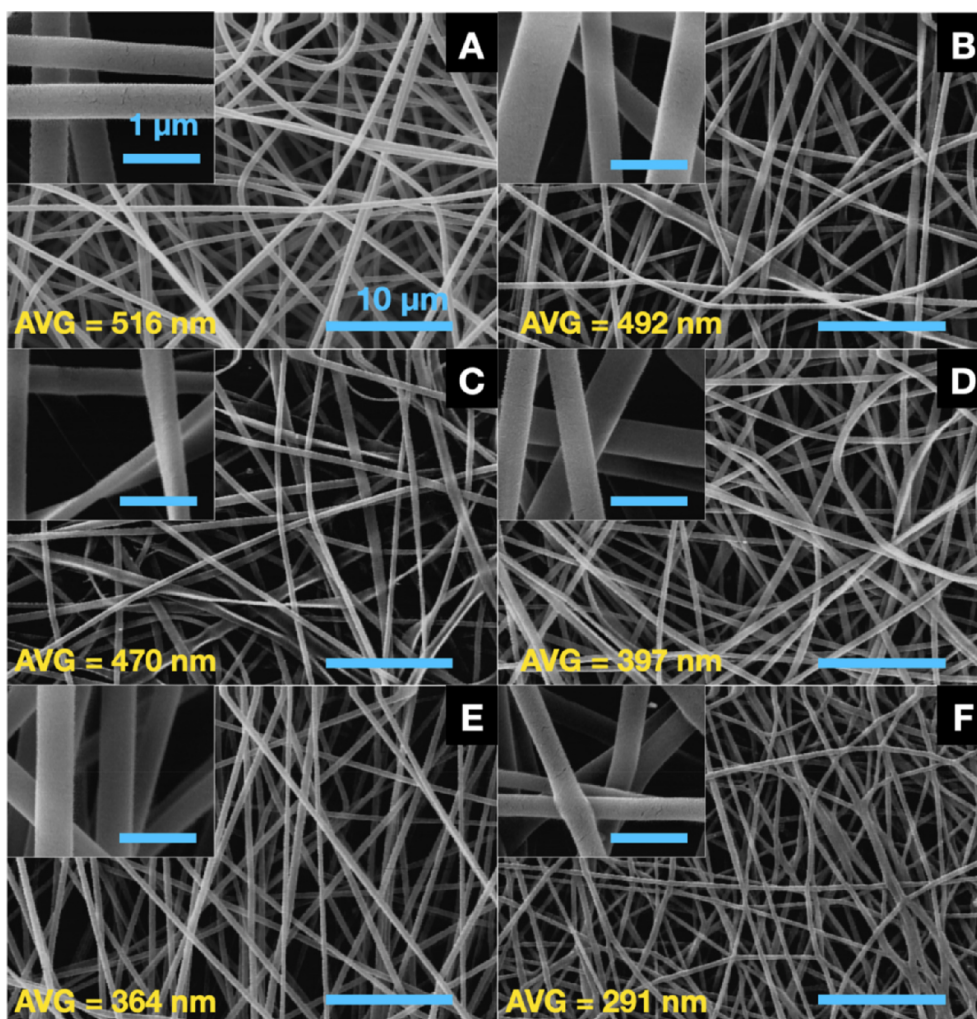


Fig. 2. Scanning electron microscope images of different scaffolds A: PVA pure, B: PVA/PEDOT(0.1), C: PVA/PEDOT(0.3), D: PVA/PEDOT(0.6), E: PVA/PEDOT(1), and F: PVA/PEDOT(3). Scale bars in large and small images equal to 10 μm and 1 μm , respectively. As mentioned earlier, increasing the amount of PEDOT:PSS in the samples decreases the mean diameter of the fibers.

the stretching of C=C in aromatic ring of PSS [7]. The peaks at 810 cm^{-1} in PEDOT-containing scaffolds and at 785 cm^{-1} in PEDOT:PSS sample are related to bending of C-H bond [7,37]. And finally, the peaks at 740 cm^{-1} in PEDOT-containing scaffolds and at 710 cm^{-1} in PEDOT:PSS scaffold are related to C-S bond in thiophene ring [38,39].

FTIR analysis results have shown that the peaks related to PVA and PEDOT:PSS were distinguishable, however as PEDOT is in very low concentrations and considering the overlapping peaks in fingerprint

zone, it was really difficult to find any chemical reactions between different components of the composite reactions.

3.3. Electrical conductivity of the scaffolds

In order to evaluate the impact of conductive polymer content on electrical properties of dry electrospun substrates, electrical conductivity of electrospun mats has been measured. In this regard, I-V curves have been drawn using the results from the Keithley multimeter,

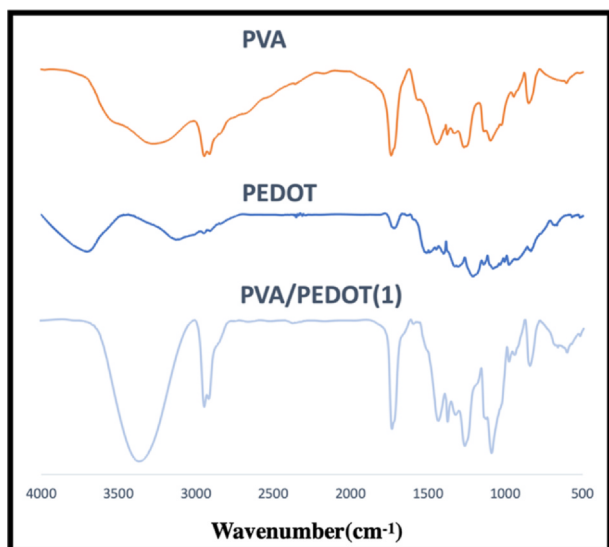


Fig. 3. FTIR spectrum of PVA, PEDOT and PVA/PEDOT(1) scaffold samples. Peaks around 3125, 1680 and 1510 cm^{-1} are respectively related to stretching of O-H in aromatic PSS ring, C = C stretching in thiophene ring and C = C stretching in aromatic PSS ring, which represent the presence of PEDOT:PSS in the structure.

and the respecting slope for the curve was used in Eq. (1) to calculate conductivity values [7]. Results on conductivity of samples is shown in Table 3.

PVA itself is insulating [40,41], however, increasing the content of conductive PEDOT into in PVA/PEDOT composites has resulted in increasing the conductivity of scaffolds. Polymers with an electrical conductivity of $< 10^{-5}$ S/m are counted as insulators [7,42]. All samples containing PEDOT in this study have electrical conductivity greater than 10^{-5} S/m and fall within the range of semiconductor materials.

There are two ways to increase electrical conductivity in non-conductive polymers during the electrospinning process. Coating fibers with conductive materials or adding conductive components to the electrospinning solutions [43]. The presence of conductive polymers in the spun nanofibers reduces the energy gap between the conduction and the valence band. As the energy of the gap decreases, the electrons move easier from the valence band to the conduction band. The holes created in the valence layers are filled by the motion of electrons. This process creates electrical conductivity in the polymer chain [42].

Another mechanism for explaining the reason for the increased conductivity relates to the single σ and double π - bonds in the conductive polymers chain. The continuous overlap of the pz-orbital zones in the double π - bonds causes the electron transfer in the carbon chain of the conductive polymers [18,42,43]. In this regard, PEDOT is highly recommended as a conductive polymer with good thermal stability over other polymers [18,43]. Electrochemical behavior of conductive polymers relies on doping which can highly influence their conductivity. PPy which is widely used in other studies for culture of neural cells can lose conductivity and become an insulator in reducing environment. On the other hand, PEDOT stays conductive in various electrochemical conditions [44]. Therefore, many studies have used PEDOT in blends or as a coating for fabrication of conductive scaffolds. Hydrogel scaffolds containing 1-3 wt% PEDOT:PSS showed to have better conductivities (2×10^{-3} – 7×10^{-3} S/m) as compared to collagen scaffolds (unmeasurable) [45]. Adding 1 wt% of PEDOT:PSS to CS/PVA electrospun scaffolds have increased the conductivity from 6×10^{-5} to 7.6×10^{-3} S/m [7]. Ostrakhovitch et al. have shown that surfaces coated by PEDOT:PEG and electrodeposited PEDOT:PSS can have up to 2.63×10^{-3} S. cm^{-2} and 1.89×10^{-2} S. cm^{-2} respectively (conductance per surface area) [44]. PEDOT can be used in hybrid scaffolds together with other

Table 3

Mechanical properties (indicated by Young's modulus, elongation at break and ultimate strength), electrical conductivity and static contact angle of different electrospun scaffolds.

Sample	Young's Modulus (MPa)	Ultimate strength (MPa)	Electrical conductivity (S/m)	Static Contact Angle (°)
PVA	61 ± 8	14.2 ± 2.8	–	64 ± 9
PVA/ PEDOT(0.1)	71 ± 9	7.2 ± 1.3	1.6×10^{-4}	52 ± 7
PVA/ PEDOT(0.3)	76 ± 11	7.6 ± 1.1	4×10^{-4}	48 ± 8
PVA/ PEDOT(0.6)	92 ± 9	8.7 ± 2.8	6×10^{-4}	45 ± 3
PVA/ PEDOT(1)	87 ± 13	9.2 ± 1.3	1×10^{-3}	43 ± 4
PVA/ PEDOT(3)	58 ± 16	9.6 ± 1.6	2×10^{-3}	32 ± 4

conductive components. Addition of 15% PEDOT to reduced graphene oxide microfibers have improved the conductivity from 1.51 S/cm up to 2.52 S/cm followed by enhanced neural differentiation of MSCs [46].

Functionality of neural cells depends on transmission of electrical signals. Therefore, conductive scaffolds can help the engineered tissue to acquire the functionality by mimicking the native environment of neural tissue. Conductivity of neural tissue is reported to range between 8×10^{-4} to 4×10^{-2} S/m in different areas [5,47]. Other researches showed that conductivity of gray matter and white matter are 0.033 and 0.022 S/m respectively [48]. Considering these values, our results on PVA/PEDOT(3) and PVA/PEDOT(1) scaffolds with 2×10^{-3} and 1×10^{-3} S/m, demonstrate the closest conductivity values to the conductivity of neural tissue. In fact, adding 3 wt% of PEDOT to pure PVA scaffolds have resulted in increasing the conductivity by 100-times. These values of scaffold conductivity can also be useful for culture of MSCs due to the closeness to the conductivity of bone marrow environment (0.15–0.02 S/m).

3.4. Topological properties of the scaffolds

Laser scanning digital microscope Images were taken from central areas of scaffolds using Olympus-OLS4100 device at 100X magnification; 2D images are also shown in Fig. 4 and Figure S4. In order to explore the surface roughness parameters, surface topography analysis was performed using OLS4100 offline V3.1.1 software and surface topography parameters—including R_a^2 , S_q^3 , V_{vc}^4 , V_{vv}^5 —are shown in Table 4.

The data in Table 4 indicates that the highest values of surface and line roughness, in terms of S_q and R_a and also void volumes amount (V_{vv} , V_{vc}), are related to PVA/PEDOT(1) sample. The presence of 1% PEDOT in this sample results in an increase of 30%, 25% and 100% in S_q , V_{vc} and V_{vv} terms, respectively, compared to PVA sample (P value ≤ 0.05). In fact, presence of conductive components in electrospinning solution can promote the randomness in deposition of fibers on foil, causing the formation of complicated patterns of fibers [7]. Although in PVA/PEDOT(3) samples, formation of thinner fibers is more dominant in moderating the surface roughness than the influence of other factors, the PVA/PEDOT(3) sample still shows better results compared to PVA sample in terms of roughness factors.

The importance and role of roughness factors in cell adhesion and growth have been emphasized previously. Surfaces with more roughness facilitate the attachment of cells and accumulate more culture media for cells. The degree of protein uptake on polymer surfaces is related to the roughness in a direct linear relationship [49,50]. Neural cells respond to rough and randomly-oriented fibers by forming short neurites [50,51]. In previous researches, it was shown that nanofibers

² Arithmetic mean height on line

³ Root mean squared height

⁴ Void volume of the core section

⁵ Void volume of the valley section

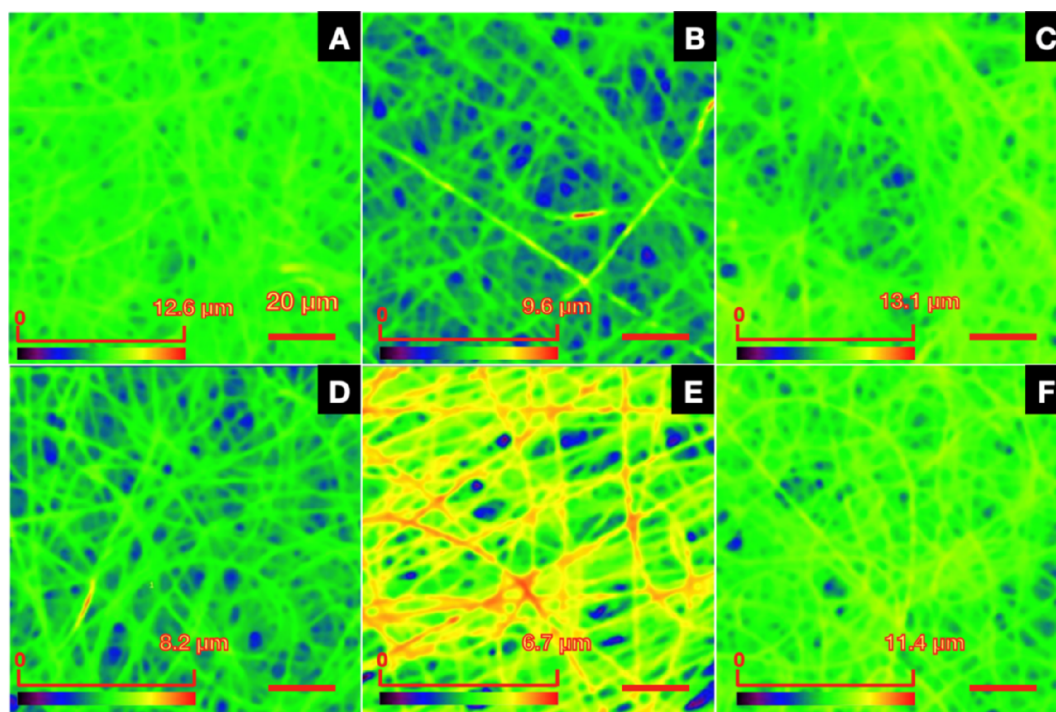


Fig. 4. Laser scanning microscopic images of topography of different surfaces: A: PVA pure, B: PVA/PEDOT(0.1), C: PVA/PEDOT(0.3), D: PVA/PEDOT(0.6), E: PVA/PEDOT(1), and F: PVA/PEDOT(3). PVA/PEDOT(1) scaffolds have the largest Ra, Sa and Vvv among all scaffolds.

Table 4

Surface topography data of different electrospun scaffolds.

Sample	Ra[nm]	Sq[μm]	Vvc[μm ³ /μm ²]	Vvv[μm ³ /μm]
PVA	24 ± 208	0.580	0.775	0.072
PVA/ PEDOT(0.1)	20 ± 217	0.600	0.779	0.098
PVA/ PEDOT(0.3)	25 ± 212	0.338	0.432	0.101
PVA/ PEDOT(0.6)	31 ± 213	0.575	0.810	0.121
PVA/ PEDOT(1)	61 ± 287	0.750	0.965	0.145
PVA/ PEDOT(3)	28 ± 229	0.622	0.801	0.110

with 500 nm of diameter and 200 nm of groove spacing can have better filament density and promote the regeneration of neural tissue *in vivo*. Other studies showed that scaffolds with 400 nm of fiber diameter can promote the growth of neurites and neural differentiation of embryonic stem cells. It was also shown that thinner fibers can promote growth of neurites [51]. In this regard, PVA/PEDOT(1) have the largest space (close to 200 nm) between valleys as compared to other scaffolds, which is similar to previous studies. Also, the diameter of fibers in PVA/PEDOT(1) and PVA/PEDOT(3) samples are close to 400 nm, which was also suggested for engineering of neural tissues.

3.5. Mechanical properties of the scaffolds

In order to evaluate the mechanical properties of samples, scaffolds have been tested using universal tensile testing machine and results, in terms of young modulus and tensile strength, are shown in Table 3 and testing curves are shown in Figure S5. Pure PVA scaffolds has better tensile strength, as compared to samples with PEDOT:PSS. For example, adding 0.1%wt PEDOT to pure PVA scaffolds results in a decrease of tensile strength from 14.2 MPa to 7.2 MPa. PEDOT is known for its superior electrical and thermal properties [7,52]. However, in terms of tensile properties, PEDOT—due to its chemical structure and presence of thiophene ring—is known as a brittle polymer with high young modulus and low mechanical strength [52,53]. Adding PEDOT to the homogeneous structure of PVA causes a decline in the tensile strength of polymeric scaffolds as compared to pure PVA samples. Also, higher

PEDOT content have led to lower elongation at break in samples (see Figure S5). In this regard, Chen et al. on PVA/PEDOT:PSS films have shown that these samples with < 10%wt PEDOT:PSS show irregular shapes in their morphology, which fades away gradually as the PEDOT:PSS content increases to up to 40%wt.

In low contents of PEDOT:PSS, cracks formed in the structure of PEDOT penetrates into PVA structure and cause a more brittle fracture [52]. In this experiment, by increasing the PEDOT content from 0.1% up to 1%wt, young modulus has increased gradually. Also, tensile strength in PEDOT-containing samples shows a gradual 33% increase from PVA/PEDOT(0.1) to PVA/PEDOT(3) sample. In PEDOT-containing scaffolds, enhanced mechanical properties of scaffolds by increasing the PEDOT content can be a result of improved crystallinity, decrease in structural defects and decrease in the diameter of fibers [7,54,55]. In fact, in thicker fibers, structural defects can form and propagate easier than thinner fibers [7].

3.6. Hydrophilicity of the scaffolds

Hydrophilicity of cross-linked electrospun scaffolds has been evaluated using a water contact angle (WCA) measurement device. Results (average ± standard deviation) have been reported in the form of average contact angle with standard (Table 3 and Figure S6). It is worth mentioning that all surfaces are highly hydrophilic in a way that drops would absorb fully in the scaffolds in less than a minute. Therefore, all results in this section are the initial contact angle values.

It is noticeable that increasing the PEDOT content in the composition results in higher hydrophilicity, as indicated by lower WCA values, where the WCA values have dropped from 64° to 43° and 32° from PVA sample to PVA/PEDOT(1) and PVA/PEDOT(3) samples, respectively (p value ≤ 0.05). PVA is a hydrophile polymer and electrospun fibers containing PVA can absorb large amounts of water in a short time [56]. Moreover, PEDOT is also a hydrophile in a way that the PEDOT used in this study was in the form of an aqueous solution. PEDOT-coated electrospun fibers are super hydrophilic, which makes it impossible to measure their static WCA. Another study on CS/PVA/PEDOT

nanofibers also mentioned that adding PEDOT to CS/PVA scaffolds can enhance the hydrophilicity of surfaces, leading to a significant increase in the cells adhesion and spreading degree of MSCs (7).

Aside from the surface chemistry, morphology of fibers and topography of the surface can also be a crucial factors in determining the wettability of the surface [7,57]. In the PVA/PEDOT(3) and PVA/PEDOT(1) samples, we have the highest reduction in fiber diameter compared to PVA sample, which leads to an increase in the specific surface area and more exposed polar and hydrophilic polymers bonds, like O-H, to the water droplet [57]. On the other hand, according to theoretical support for the Wenzel Equation (Eq. (2)), water contact angle depends on the equilibrium between surface energies of solid-liquid (γ_{sl}), solid-gas (γ_{sv}), liquid-gas (γ_{lv}) and real area/planar area (r_w) index [58]. Therefore, when there are more polar bonds at the surface, they lead to bonding to water molecules. This reduces the amount of the γ_{sl} s, thus reducing the contact angle, according to Eq. (2); also, r_w amount represents roughness and in smooth surfaces is ($r_w = 1$), but with the increase in roughness factors as well as surface grooves, this index tends to be greater than 1 ($r_w \gg 1$). With due attention to Wenzel equation (Eq. (2)), this results in decrease of contact angle, especially in confirming the results of the PVA/PEDOT(1) sample [57,58]. Essentially, in micro/nano-fibrous structures, thinner fibers and higher roughness will increase the solid-liquid interface, meanwhile if the fibers are hydrophilic, water will have more tendency to be absorbed into the structure of fibers [7,57].

$$\cos\theta = \frac{\gamma_{sv} - \gamma_{sl}}{\gamma_{lv}} * r_w \quad (2)$$

where r_w is real area/planar area, γ_{sl} is surface energies of solid-liquid, γ_{sv} is surface energies of solid-gas and γ_{lv} is surface energies of liquid-gas.

3.7. Biological properties of the scaffolds

In order to understand the morphological alterations of seeded MSCs and investigation of cell attachment and spreading on the scaffolds, cells were grown on different groups. At the end of day 1 and day 7, cells were fixed and SEM images were acquired (see Figure S7 for cell attachments at day 1 and Fig. 5 for cell spreading at day 7). These images are demonstrating that addition of PEDOT will result in better attachment of cells as depicted by higher population of cells in closer contact. In the next few days, cells have grown and higher populations with smaller distances are observable in day 7 images of Fig. 5. Although on day 1 PVA/PEDOT(3) surfaces showed the best support for cell attachment, on day 7, largest cell areas belonged to PVA/PEDOT(1) surfaces, where surface roughness parameters were the highest among all the other scaffolds. Improved cell attachment in PVA/PEDOT(1) and PVA/PEDOT(3) surfaces can be due to the proper hydrophilicity of these surfaces.

In previous studies it was reported that nano-roughness of $20 \text{ nm} < R_a < 100 \text{ nm}$ and $20 \text{ nm} < R_a < 50 \text{ nm}$ can promote the adhesion and growth of rat cortical neurons and MSCs, respectively, which are in consent with our results [51].

Other factors influencing the growth of cells on electrospun fibers are fiber diameter and fiber orientation. Cells have the tendency to grow in the direction of topographical features of the surface. This tendency has been numerous reported in different studies on the growth of cells on aligned electrospun fibers. The same behavior is also happening on randomly oriented electrospun fibers. MSCs behave differently on nano-scale and micro-scale fibers. Nuclear structure and cytoskeletal filaments of MSCs can grow preferentially in the direction of fibers [7,51]. It has already been shown that cultured cells on cylindrical fibers tend to form a certain curvature by the cell membrane to reduce their free energy, and the diameter of the fibers in the range of 320–500 nm is very suitable for this purpose [59]. Our results show that electrospun scaffolds with average diameters of 350 nm on PVA/

PEDOT(1) sample have the best support for growth and spreading of MSCs.

Evaluation of metabolic activity of seeded cells through MTT is shown in Fig. 6. Comparing the O.D. results of different samples in a 7-day period shows that all scaffold samples have better support for viability and growth of cells. Samples on PVA/PEDOT(3) surfaces have the best O.D. results at day 1. Due to the fact that the doubling time for MSCs is almost 2 days [7,60], proliferation of MSCs in the first 24 h should be negligible. Therefore, O.D. in PVA/PEDOT(3) surfaces after 24 h represents the better support for cell attachment on these surfaces. In this regard, previous studies have also shown the enhancement of cell adhesion on conductive scaffolds [61,62].

All scaffolds show an increasing trend in O.D. from day 1 to day 7, which represent their growing pattern on scaffolds. Although PVA/PEDOT(3) scaffold showed promising results for O.D. in day 1, the growth of cells on this scaffold was significantly lower than other samples. This could be due to the toxicity of high amounts of PEDOT:PSS. Previous reports on bone tissue engineering using conductive scaffolds based on gelatin/bioactive glass showed that scaffolds containing more than 0.6 wt% PEDOT can cause toxicity for MSCs [7,63]. On the other hand, comparing the O.D. values between PVA and PVA/PEDOT(0.1) shows that presence of small amounts of PEDOT can result in better viability of MSCs. As the topographical parameters between PVA and PVA/PEDOT(0.1) are similar, this change in O.D. values might be due to the variations in surface chemistry, where presence of conductive components can enhance cell signaling and promote the adsorption of surface proteins, e.g. fibronectin [22,60,64–66]. Also, proliferation of stem cells when grown on conductive scaffolds was improved [62,67,68]. Similarly, our results have shown an increasing trend in the O.D. results, especially for PVA/PEDOT(1) sample, which shows the proper support of these surfaces for stem cell growth, and considering the attachment and morphology images of these surfaces, this composition of scaffold has been selected for further differentiation experiments. It is worth mentioning that using glutaraldehyde as a crosslinking agent did not result in a cytotoxicity of scaffolds during the 7-day culture period. Similar to this, other studies have shown that glutaraldehyde could be used as a crosslinking agent with minimized cytotoxic response [69,70]. Aside from that, glycine can be further used to block the toxic aldehyde groups [7,70,71].

3.8. Neural differentiation and gene expression

In order to evaluate the neural differentiation of cells, expression of some neural markers—including nestin, β -tubulin III and enolase—were analyzed using real-time PCR method, with the results being normalized to negative control samples (undifferentiated cells).

Nestin is a microfilament in neural progenitor cells and, therefore, is an early neural differentiation marker [4,72–74]. β -tubulin III is a microtubule that is exclusively found in neurons and testis cells, thus is another important neural marker in late neural differentiation [75–78]. Therefore, upregulation of these genes can show the progress in induction of neural differentiation in all differentiation groups including TCP + DM, Scaffold + DM and Scaffold + DM + ES samples (see Table 2 for details on groups and relative treatments).

Differentiation protocol in this study uses different chemical factors, including RA, Forskolin and IBMX. These three factors have been previously studied and shown to be promising in induction of neural differentiation using different types of stem cells [79–81]. RA either solely, or in combination of other differentiation or survival promotion factors have been extensively used for induction of neural differentiation [79,82–83]. Induction with RA results in improved formation of neurites both in number and length [84]. In a study on neural differentiation of hESCs, adding RA increased nestin expression by 56% and 67% in day 7 and day 14, respectively [79]. MSCs treated with 30 μM of RA have indicated the expression of neuron-specific markers and formation of synaptic connections [85]. However, some studies have

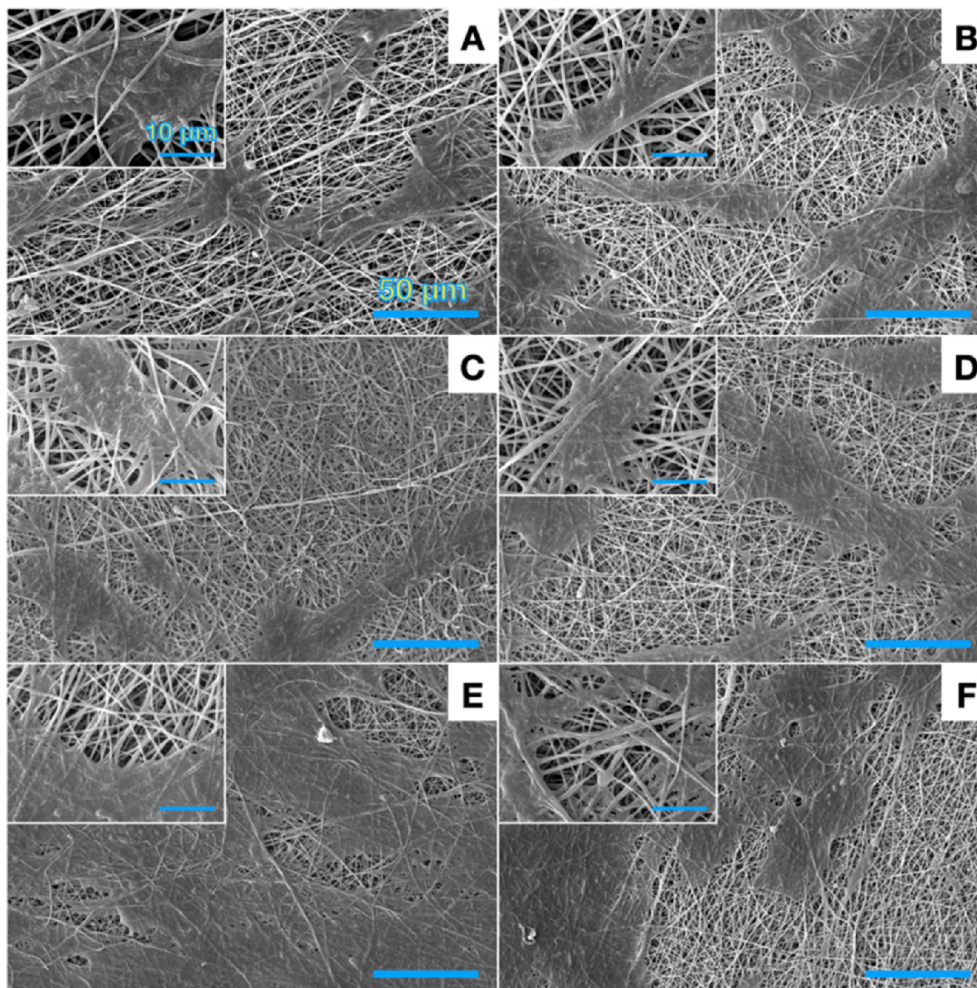


Fig. 5. SEM imaging of cell spreading after 7 days of culture: A: PVA pure, B: PVA/PEDOT(0.1), C: PVA/PEDOT(0.3), D: PVA/PEDOT(0.6), E: PVA/PEDOT(1), and F: PVA/PEDOT(3). Cells have shown better growth on PEDOT containing scaffolds. PVA/PEDOT(1) scaffold have shown the best cell area compared to other cells. Scale bars in large and small images are equal to 50 µm and 10 µm, respectively.

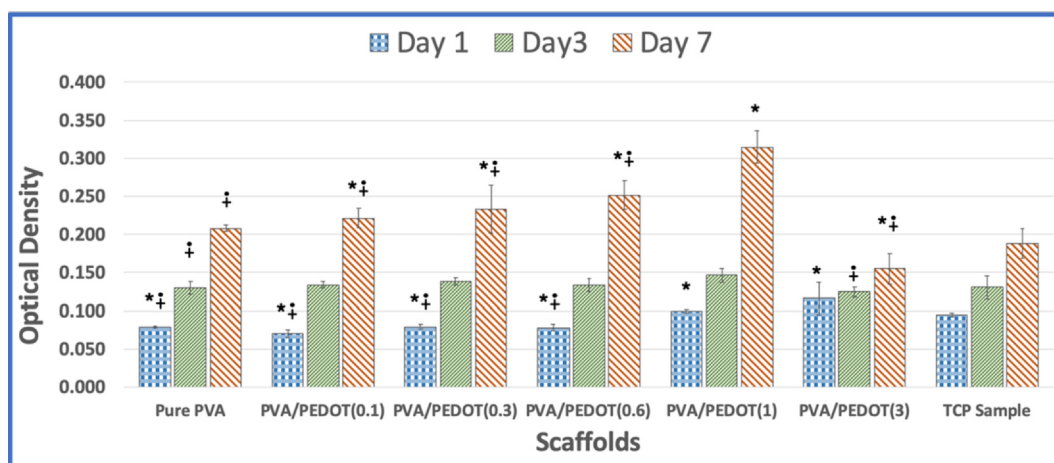


Fig. 6. MTT assay for MSC viability on different nanofibrous scaffolds and TCP. The * & † signs indicate the significance (p-value < 0.05) as compared to TCP and PVA/PEDOT(1) samples. Scaffold samples have shown better support for cell adhesion and growth. PVA/PEDOT(1) scaffold have shown the best support for cell viability after 7 days of culture without any sign of cytotoxicity. It should be noted that not all the significant samples have been marked.

shown that induction with RA alone does not result in formation of mature neuronal phenotype and morphology [86]. Therefore, many studies have used RA along with other differentiation factor to improve neural differentiation factors including Forskolin and IBMX [79,82,87].

Aside from RA, Forskolin and IBMX can influence the early neural-like differentiation and change of morphology of MSCs through activation of cyclic adenosine monophosphate (cAMP) and suppressing neuron restrictive silencer factor (NRSF) [81,84,88]. In induction of human

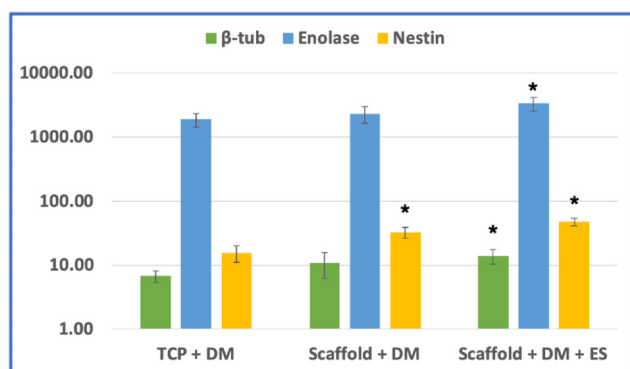


Fig. 7. Expression of neural marker genes in different differentiation treatments. Cells cultured on TCP samples (TCP + DM), scaffolds (Scaffold + DM) and incorporation of a conductive scaffold and electrical stimulation (Scaffold + DM + ES) have been analyzed for expression of neural markers β -tub, Enolase and Nestin (see table 2 for details on groups and relative treatments). Gene expression results were normalized as compared to untreated TCP samples (control). Incorporation of a conductive scaffold and electrical stimulation have resulted in increased expression of neural differentiation genes including Nestin and β -tubulin III. The * sign indicates that the values of the samples are significant compared to the TCP + DM values, (p-value < 0.05).

MSCs, it was shown that IBMX can be a more crucial factor in formation of neurites as compared to other differentiation factors including RA, cAMP, bFGF and NGF [89]. Previous studies have shown the promise of using either RA or Forskolin and IBMX together with knock-out of serum in differentiation of induced pluripotent stem cells [90]. Therefore, as various factors including RA, Forskolin and IBMX promote the different stages of neural differentiation [84,90], in this study a mixture of these factors together with step-wise knock-out of serum were used for chemical induction of neural differentiation. Gene expression results have shown that using the differentiation media alone can cause overexpression of neural markers including Enolase, Nestin and β -tubulin in all differentiation samples. Moreover, light microscopy images of differentiating and undifferentiated cells (control group) on TCP have shown the promise of differentiation media in formation of neurites in Scaffold + DM group (Figure S8 - images for scaffolds samples are not shown).

In the Scaffold + DM sample, expression of nestin increased by 2-times (p value ≤ 0.05) compared to TCP + DM sample which indicates the potential of using conductive scaffolds in neural induction of BM-MSCs (see Fig. 7). Aside from that, expression of enolase has also increased in Scaffold + DM + ES and Scaffold + DM samples as compared to TCP + DM sample, however, the changes in expression were not statistically significant. Moreover, in Scaffold + DM + ES sample, expression of nestin and β -tubulin III have increased by 3- and 2-times respectively as compared to TCP + DM sample. Moreover, nestin gene expression in the Scaffold + DM + ES sample was 1.5-times that of the Scaffold + DM sample. These results clearly shows the influence of incorporating electrical stimulation with conductive scaffolds for neural differentiation. Although the mechanisms behind the influence of conductive scaffolds and electrical stimulation on neural differentiation and nerve regeneration are not yet fully understood, some possible postulations include altered adsorption of proteins and electrophoretic redistribution of cell surface receptors [2,91,92].

One of the main challenges in designing scaffolds for excitable tissues, including neural and cardiac tissue, is to reach an electrical microenvironment for cells capable of mimicking electrical signal transmission [93]. Considering the functionality of neural cells in terms of their electrochemical activities, it is not far from expectation that conductive scaffolds and incorporation of electrical stimulation have enhanced the maturation and functionality of neuron-like cells [18,26,94]. In this regard, rat nerve stem cells and PC-12 cells have

shown improved extension of neurites and elongation of cell area while subjected to electrical stimulation on conductive scaffolds [67 95-97]. Wang et al. have shown that aligned conductive scaffolds can be highly beneficial in reaching polarity of cells on neural cells [98]. Moreover, Puladzadeh et al. have indicated the promise of incorporation of conductive scaffolds with electromagnetic stimulation in improved expression of neural markers. It was shown that while using electromagnetic stimulation, MAP2, a neuron-specific marker related to cytoskeleton proteins have overexpressed for at least 4-fold on conductive scaffolds compared to un-conductive samples. In addition to that, β -tubulin upregulated by more than 2-fold as a result of the electromagnetic field, whereas using conductive scaffolds did not have any significant influence on the expression of this gene after 2 weeks of culture [62]. Rahmani et al. have shown that MSCs cultured on conductive scaffolds will have a better expression of neural markers including MAP-2, β -tubulin and nestin when treated with 100 Hz of alternating current (AC) rather than lower frequencies (0.1 Hz) [99]. Other studies have shown that expression of neural genes including NGF, GAP43 and SYP in PC-12 cells grown on conductive surfaces will upregulate by more than 5-fold [68,100]. Other studies with graphene and PEDOT have also shown the importance of incorporating conductive scaffolds with electrical stimulation for enhanced expression of neuronal markers, especially Tuj-1, in protein level [46,101]. Ostrakhovitch et al. have shown that surfaces made of PEDOT:PEG and PEDOT:PSS can improve the β -tubulin expression in P19 embryonic carcinoma cells and induce neural differentiation even at the absence of RA [44]. Our findings on upregulation of neural gene are in accordance with previous researches on the influence of conductive scaffolds and electrical stimulation for enhancing *in-vitro* neural induction for stem cells. Although further studies should investigate the mechanisms involved in improvement of neural induction through conductive scaffolds and electrical stimulation, these results indicate that incorporation of our conductive scaffolds with electrical stimulation provide a better neural induction for rat BM-MSCs.

4. Conclusions

In this study, PVA scaffolds were made with different weight percentages of PEDOT, and their properties were optimized to mimic the environment of neural tissue. Our results show that PVA scaffolds containing 1 wt% of PEDOT can be very effective in enhancing the electrical conductivity of the nonconductive polymers, simultaneously improving the topographic and morphological properties of the fibers. Also, PEDOT-containing scaffolds, especially PEDOT/PVA (1), have resulted in enhanced metabolic activity of MSCs. Also, our results regarding neural differentiation of MSCs demonstrates that induction of electrical stimulation on PEDOT-containing conductive scaffolds in the presence of differentiation factors—including RA, IBMX and Forskolin—can improve the expression of neuronal genes. Finally, our results suggest that using PEDOT as a conductive component in fabrication of neural tissue engineering scaffolds can be useful in improving physical properties of scaffolds and enhance the neural differentiation of stem cells.

Funding

The authors received no specific funding for this work.

Ethical approval

All applicable international, national, and/or institutional guidelines for the care and use of animals were followed.

Declaration of Competing Interest

The authors declare that they have no known competing financial interests or personal relationships that could have appeared to influence the work reported in this paper.

Acknowledgements

Authors would like to express their great appreciation to Erfan Dashti-Moghaddam in Marquette University, and Simzar Hosseinzadeh, Samaneh Mirzaei, Fatemeh Jamshidi-Adeghani, Saeid Vakilian, Ali Hosseini Rad and Ali Naderi Sohi in Stem Cell Technology Research Center, and Mehri Marvi, Saeed Rafizadeh-Tafti, Hafez Jafari, Jhamak Noormohammadi and Saba Aslani in University of Tehran, and Reza Lashkarolouki in Tehran Polytechnic.

Appendix A. Supplementary material

Supplementary data to this article can be found online at <https://doi.org/10.1016/j.eurpolymj.2020.110051>.

References

- [1] H. Cao, T. Liu, S.Y. Chew, The application of nanofibrous scaffolds in neural tissue engineering, *Adv. Drug Deliv. Rev.* 61 (12) (2009) 1055–1064.
- [2] A. Subramanian, U.M. Krishnan, S. Sethuraman, Development of biomaterial scaffold for nerve tissue engineering: Biomaterial mediated neural regeneration, *J. Biomed. Sci.* 16 (1) (2009) 108.
- [3] F. Yang, R. Murugan, S. Wang, S. Ramakrishna, Electrospinning of nano/micro scale poly (L-lactic acid) aligned fibers and their potential in neural tissue engineering, *Biomaterials* 26 (15) (2005) 2603–2610.
- [4] M. Zare, M. Soleimani, A. Akbarzadeh, B. Bakhshandeh, S.H. Aghaee-Bakhtiari, N. Zarghami, A Novel Protocol to Differentiate Induced Pluripotent Stem Cells by Neuronal microRNAs to Provide a Suitable Cellular Model, *Chem Biol Drug Des.* 86 (2) (2015) 232–238.
- [5] P. Zarrintaj, B. Bakhshandeh, I. Rezaeian, B. Heshmatian, M.R. Ganjali, A Novel Electroactive Agarose-Aniline Pentamer Platform as a Potential Candidate for Neural Tissue Engineering, *Sci Rep.* 7 (1) (2017) 17187.
- [6] A. Babaie, J. Lumicisi, H. Thissen, P.-Y. Wang, H. Sumer, P. Kingshott, Binary Colloidal Crystal (BCC) Substrates for Controlling the Fate of Mouse Embryonic Stem Cells, *Biointerfaces, Colloids and Surfaces B*, 2020.
- [7] A. Abedi, M. Hasanazadeh, L. Tayebi, Conductive nanofibrous Chitosan/PEDOT: PSS tissue engineering scaffolds, *Mater. Chem. Phys.* 237 (2019) 121882.
- [8] T. Bini, S. Gao, X. Xu, S. Wang, S. Ramakrishna, K.W. Leong, Peripheral nerve regeneration by microbraided poly (L-lactide-co-glycolide) biodegradable polymer fibers, *J. Biomed. Mater. Res. Part A Off. J. Soc. Biomater. Japanese Soc. Biomater. Australian Soc. Biomater. Korean Soc. Biomater.* 68 (2) (2004) 286–295.
- [9] C.-J. Chang, S.-H. Hsu, The effects of low-intensity ultrasound on peripheral nerve regeneration in poly (DL-lactic acid-co-glycolic acid) conduits seeded with Schwann cells, *Ultrasound Med. Biol.* 30 (8) (2004) 1079–1084.
- [10] M.R. Abidian, J.M. Corey, D.R. Kipke, D.C. Martin, Conducting-polymer nanotubes improve electrical properties, mechanical adhesion, neural attachment, and neurite outgrowth of neural electrodes, *small* 6 (3) (2010) 421–429.
- [11] Matysiak W, Tański T, Smok W, editors. *Electrospinning as a Versatile Method of Composite Thin Films Fabrication for Selected Applications. Solid State Phenomena*; 2019: Trans Tech Publ.
- [12] C. Wang, J. Wang, L. Zeng, Z. Qiao, X. Liu, H. Liu, et al., Fabrication of electrospun polymer nanofibers with diverse morphologies, *Molecules* 24 (5) (2019) 834.
- [13] N. Ashammakhi, A. Ndreu, Y. Yang, H. Ylikauppi, L. Nikkola, Nanofiber-based scaffolds for tissue engineering, *Eur. J. Plast. Surg.* 35 (2) (2012) 135–149.
- [14] Z. Ma, M. Kotaki, R. Inai, S. Ramakrishna, Potential of nanofiber matrix as tissue-engineering scaffolds, *Tissue Eng.* 11 (1–2) (2005) 101–109.
- [15] M. Mehrali, A. Thakur, C.P. Pennisi, S. Talebian, A. Arpanaei, M. Nikkha, et al., Nanoreinforced hydrogels for tissue engineering: Biomaterials that are compatible with load-bearing and electroactive tissues, *Adv. Mater.* 29 (8) (2017) 1603612.
- [16] J.B. Veluru, K. Satheesh, D. Trivedi, M.V. Ramakrishna, N.T. Srinivasan, Electrical properties of electrospun fibers of PANI-PMMA composites, *J. Eng. Fibers Fabr.* 2 (2) (2007) 155892500700200203.
- [17] A. Zaszczynska, P. Sajkiewicz, A. Grady, Piezoelectric Scaffolds as Smart Materials for Neural Tissue Engineering, *Polymers* 12 (1) (2020) 161.
- [18] L. Ghasemi-Mobarakeh, M.P. Prabhakaran, M. Morshed, M.H. Nasr-Esfahani, H. Baharvand, S. Kiani, et al., Application of conductive polymers, scaffolds and electrical stimulation for nerve tissue engineering, *Journal of tissue engineering and regenerative medicine* 5 (4) (2011) e17–e35.
- [19] X.T. Cui, D.D. Zhou, Poly (3,4-ethylenedioxythiophene) for chronic neural stimulation, *IEEE Trans. Neural. Syst. Rehabil. Eng.* 15 (4) (2007) 502–508.
- [20] X. Cui, D.C. Martin, Electrochemical deposition and characterization of poly(3,4-ethylenedioxythiophene) on neural microelectrode arrays, *Sens. Actuat. B* 89 (1–2) (2003) 92–102.
- [21] A. Peramo, M.G. Urbanczek, S.A. Spanninga, L.K. Povlich, P. Cederna, D.C. Martin, In situ polymerization of a conductive polymer in acellular muscle tissue constructs, *Tissue Eng. Part A* 14 (3) (2008) 423–432.
- [22] M.H. Bolin, K. Svennersten, X. Wang, I.S. Chronakis, A. Richter-Dahlfors, E.W. Jager, et al., Nano-fiber scaffold electrodes based on PEDOT for cell stimulation, *Sens. Actuators, B* 142 (2) (2009) 451–456.
- [23] V. Karagkiozaki, P. Karagiannidis, M. Gioti, P. Kavatzikidou, D. Georgiou, E. Georgaraki, et al., Bioelectronics meets nanomedicine for cardiovascular implants: PEDOT-based nanocoatings for tissue regeneration, *Biochim. et Biophys. Acta (BBA)-General Sub.* 1830 (9) (2013) 4294–4304.
- [24] M. Asplund, E. Thaning, J. Lundberg, A. Sandberg-Nordqvist, B. Kostyszyn, O. Inganäs, et al., Toxicity evaluation of PEDOT/biomolecular composites intended for neural communication electrodes, *Biomater. Mater.* 4 (4) (2009) 045009.
- [25] A. Kumar, S.S. Han, PVA-based hydrogels for tissue engineering: A review, *Int. J. Polymeric Mater. Polymeric Biomater.* 66 (4) (2017) 159–182.
- [26] C. Chen, X. Bai, Y. Ding, I.-S. Lee, Electrical stimulation as a novel tool for regulating cell behavior in tissue engineering, *Biomater. Research* 23 (1) (2019) 25.
- [27] Y. Huang, Y. Li, J. Chen, H. Zhou, S. Tan, Electrical stimulation elicits neural stem cells activation: new perspectives in CNS repair, *Front. Hum. Neurosci.* 9 (2015) 586.
- [28] R. Zhu, Z. Sun, C. Li, S. Ramakrishna, K. Chiu, L. He, Electrical stimulation affects neural stem cell fate and function in vitro, *Exp. Neurol.* 319 (2019) 112963.
- [29] M.O. Oftadeh, B. Bakhshandeh, M.M. Dehghan, A. Khojasteh, Sequential application of mineralized electroconductive scaffold and electrical stimulation for efficient osteogenesis, *J. Biomed Mater Res A* 106 (5) (2018) 1200–1210.
- [30] J.-H. He, Y.-Q. Wan, J.-Y. Yu, Effect of concentration on electrospun polyacrylonitrile (PAN) nanofibers, *Fibers Polym.* 9 (2) (2008) 140–142.
- [31] M.C. McManus, E.D. Boland, H.P. Koo, C.P. Barnes, K.J. Pawlowski, G.E. Wnek, et al., Mechanical properties of electrospun fibrinogen structures, *Acta Biomater.* 2 (1) (2006) 19–28.
- [32] B. Rezaei, A.M. Shoushtari, M. Rabiee, L. Uzun, A.P. Turner, M.W. Cheung, Multifactorial modeling and optimization of solution and electrospinning parameters to generate superfine polystyrene nanofibers, *Adv. Polym. Tech.* 37 (8) (2018) 2743–2755.
- [33] M. Ghanipour, D. Dorrani, Effect of Ag-nanoparticles doped in polyvinyl alcohol on the structural and optical properties of PVA films, *J. Nanomater.* 2013 (2013).
- [34] P. Tehrani, A. Kancirzewska, X. Crispin, N.D. Robinson, M. Fahlman, M. Berggren, The effect of pH on the electrochemical over-oxidation in PEDOT: PSS films, *Solid State Ionics* 177 (39–40) (2007) 3521–3527.
- [35] A.N. Aleshin, A.S. Berestennikov, P.S. Krylov, I.P. Shcherbakov, V.N. Petrov, I.N. Trapeznikova, et al., Electrical and optical properties of bacterial cellulose films modified with conductive polymer PEDOT/PSS, *Synth. Met.* 199 (2015) 147–151.
- [36] P. Khanna, N. Singh, S. Charan, V. Subbarao, R. Gokhale, U. Mulik, Synthesis and characterization of Ag/PVA nanocomposite by chemical reduction method, *Mater. Chem. Phys.* 93 (1) (2005) 117–121.
- [37] J. Jian, X. Guo, L. Lin, Q. Cai, J. Cheng, J. Li, Gas-sensing characteristics of dielectrically assembled composite film of oxygen plasma-treated SWCNTs and PEDOT/PSS polymer, *Sens. Actuat. B* 178 (2013) 279–288.
- [38] M. Kiristi, A.U. Oksuz, L. Oksuz, S. Ulusoy, Electrospun chitosan/PEDOT nanofibers, *Mater. Sci. Eng. C* 33 (7) (2013) 3845–3850.
- [39] D. Wang, Y. Bao, J.W. Zha, J. Zhao, Z.M. Dang, G.H. Hu, Improved dielectric properties of nanocomposites based on poly(vinylidene fluoride) and poly(vinyl alcohol)-functionalized graphene, *ACS Appl. Mater. Inter.* 4 (11) (2012) 6273–6279.
- [40] M.E. Nicho, H. Hu, Fourier transform infrared spectroscopy studies of polypyrrole composite coatings, *Sol. Energy Mater. Sol. Cells* 63 (4) (2000) 423–435.
- [41] T.-H. Le, Y. Kim, H. Yoon, Electrical and electrochemical properties of conducting polymers, *Polymers* 9 (4) (2017) 150.
- [42] R. Balint, N.J. Cassidy, S.H. Cartmel, Conductive polymers: Towards a smart biomaterial for tissue engineering, *Acta Biomater.* 10 (6) (2014) 2341–2353.
- [43] E.A. Ostrakhovitch, J.C. Byers, K.D. O’Neil, O.A. Semenikhin, Directed differentiation of embryonic P19 cells and neural stem cells into neural lineage on conducting PEDOT-PEG and ITO glass substrates, *Arch Biochem. Biophys.* 528 (1) (2012) 21–31.
- [44] S. Sirivisoot, R. Pareta, B.S. Harrison, Protocol and cell responses in three-dimensional conductive collagen gel scaffolds with conductive polymer nanofibers for tissue regeneration, *Interface focus* 4 (1) (2014) 20130050.
- [45] W. Guo, X. Zhang, X. Yu, S. Wang, J. Qiu, W. Tang, et al., Self-Powered Electrical Stimulation for Enhancing Neural Differentiation of Mesenchymal Stem Cells on Graphene-Poly(3,4-ethylenedioxythiophene) Hybrid Microfibers, *ACS Nano* 10 (5) (2016) 5086–5095.
- [46] L.A. Geddes, L.E. Baker, The specific resistance of biological material—a compendium of data for the biomedical engineer and physiologist, *Med. Biol. Eng.* 5 (3) (1967) 271–293.
- [47] D. Miklavcic, N. Pavšelj, F.X. Hart, *Electric properties of tissues*, Wiley Encyclopedia Biomater. Eng. (2006).
- [48] N.J. Hallab, K.J. Bundy, K. O’Connor, R.L. Moses, J.J. Jacobs, Evaluation of metallic and polymeric biomaterial surface energy and surface roughness characteristics for directed cell adhesion, *Tissue Eng.* 7 (1) (2001) 55–71.
- [49] F. Zamani, M. Amani-Tehran, M. Latifi, M.A. Shokrgozar, The influence of surface nanoroughness of electrospun PLGA nanofibrous scaffold on nerve cell adhesion and proliferation, *J. Mater. Sci. - Mater. Med.* 24 (6) (2013) 1551–1560.
- [50] A.T. Nguyen, S.R. Sathe, E.K. Yim, From nano to micro: topographical scale and its impact on cell adhesion, morphology and contact guidance, *J. Phys.: Condens. Matter* 28 (18) (2016) 183001.
- [51] C.-h. Chen, A. Torrents, L. Kulinsky, R.D. Nelson, M.J. Madou, L. Valdevit, et al.,

- Mechanical characterizations of cast Poly (3, 4-ethylenedioxythiophene): Poly (styrenesulfonate)/Polyvinyl Alcohol thin films, *Synth. Met.* 161 (21–22) (2011) 2259–2267.
- [53] S. Ichikawa, N. Toshima, Improvement of thermoelectric properties of composite films of PEDOT-PSS with xylitol by means of stretching and solvent treatment, *Polym. J.* 47 (7) (2015) 522–526.
- [54] H. Jafari, M. Shahrousvand, B. Kaffashi, Preparation and characterization of reinforced poly (ϵ -caprolactone) nanocomposites by cellulose nanowhiskers, *Polym. Compos.* 41 (2) (2020) 624–632.
- [55] S.-C. Wong, A. Baji, S. Leng, Effect of fiber diameter on tensile properties of electrospun poly (ϵ -caprolactone), *Polymer* 49 (21) (2008) 4713–4722.
- [56] J. Choi, J. Lee, J. Choi, D. Jung, S.E. Shim, Electrospun PEDOT: PSS/PVP nanofibers as the chemiresistor in chemical vapour sensing, *Synth. Met.* 160 (13–14) (2010) 1415–1421.
- [57] S. Han, R. Yang, C. Li, L. Yang, The Wettability and Numerical Model of Different Silicon Microstructural Surfaces, *Appl. Sci.* 9 (3) (2019) 566.
- [58] M.A. Hubbe, D.J. Gardner, W. Shen, Contact angles and wettability of cellulosic surfaces: A review of proposed mechanisms and test strategies, *BioResources.* 10 (4) (2015) 8657–8749.
- [59] F. Tian, H. Hosseinkhani, M. Hosseinkhani, A. Khademhosseini, Y. Yokoyama, G.G. Estrada, et al., Quantitative analysis of cell adhesion on aligned micro- and nanofibers, *J. Biomed. Mater. Res. Part A* 84 (2) (2008) 291–299.
- [60] R.H. Lee, B. Kim, I. Choi, H. Kim, H.S. Choi, K. Suh, et al., Characterization and expression analysis of mesenchymal stem cells from human bone marrow and adipose tissue, *Cell. Physiol. Biochem.* 14 (4–6) (2004) 311–324.
- [61] Z. Zhang, M. Rouabhi, Z. Wang, C. Roberge, G. Shi, P. Roche, et al., Electrically conductive biodegradable polymer composite for nerve regeneration: electricity-stimulated neurite outgrowth and axon regeneration, *Artif. Organs.* 31 (1) (2007) 13–22.
- [62] F. Pouladzadeh, A.A. Katbab, N. Haghighipour, E. Kashi, Carbon nanotube loaded electrospun scaffolds based on thermoplastic urethane (TPU) with enhanced proliferation and neural differentiation of rat mesenchymal stem cells: The role of state of electrical conductivity, *Eur. Polym. J.* 105 (2018) 286–296.
- [63] M. Yazdimamaghani, M. Razavi, M. Mozafari, D. Vashae, H. Kotturi, L. Tayebi, Biomimetic and biocompatible studies of bone conductive scaffolds containing poly (3, 4-ethylenedioxythiophene): poly (4-styrene sulfonate) (PEDOT: PSS), *J. Mater. Sci. - Mater. Med.* 26 (12) (2015) 274.
- [64] N.K. Guimard, N. Gomez, C.E. Schmidt, Conducting polymers in biomedical engineering, *Prog. Polym. Sci.* 32 (8–9) (2007) 876–921.
- [65] A. Kotwal, C.E. Schmidt, Electrical stimulation alters protein adsorption and nerve cell interactions with electrically conducting biomaterials, *Biomaterials* 22 (10) (2001) 1055–1064.
- [66] X. Niu, M. Rouabhi, N. Chiffot, M.W. King, Z. Zhang, An electrically conductive 3D scaffold based on a nonwoven web of poly (L-lactic acid) and conductive poly (3, 4-ethylenedioxythiophene), *J. Biomed. Mater. Res. Part A* 103 (8) (2015) 2635–2644.
- [67] M.P. Prabhakaran, L. Ghasemi-Mobarakeh, G. Jin, S. Ramakrishna, Electrospun conducting polymer nanofibers and electrical stimulation of nerve stem cells, *J. Biosci. Bioeng.* 112 (5) (2011) 501–507.
- [68] Y. Wu, L. Wang, T. Hu, P.X. Ma, B. Guo, Conductive micropatterned polyurethane films as tissue engineering scaffolds for Schwann cells and PC12 cells, *J. Colloid Interface Sci.* 518 (2018) 252–262.
- [69] E.S. Costa-Júnior, E.F. Barbosa-Stancioli, A.A.P. Mansur, W.L. Vasconcelos, H.S. Mansur, Preparation and characterization of chitosan/poly(vinyl alcohol) chemically crosslinked blends for biomedical applications, *Carbohydr. Polym.* 76 (3) (2009) 472–481.
- [70] K.S. Rho, L. Jeong, G. Lee, B.M. Seo, Y.J. Park, S.D. Hong, et al., Electrospinning of collagen nanofibers: effects on the behavior of normal human keratinocytes and early-stage wound healing, *Biomaterials* 27 (8) (2006) 1452–1461.
- [71] E. Gendler, S. Gendler, M.E. Nimni, Toxic reactions evoked by glutaraldehyde-fixed pericardium and cardiac valve tissue bioprosthesis, *J. Biomed. Mater. Res.* 18 (7) (1984) 727–736.
- [72] K. Michalczyk, M. Ziman, Nestin structure and predicted function in cellular cytoskeletal organization, *Histol. Histopathol.* (2005).
- [73] D. Park, A.P. Xiang, F.F. Mao, L. Zhang, C.G. Di, X.M. Liu, et al., Nestin is required for the proper self-renewal of neural stem cells, *Stem cells.* 28 (12) (2010) 2162–2171.
- [74] L. Xie, X. Zeng, J. Hu, Q. Chen, Characterization of nestin, a selective marker for bone marrow derived mesenchymal stem cells, *Stem Cells Int.* 2015 (2015).
- [75] M.W. Breuss, I. Leca, T. Gstrein, A.H. Hansen, D.A. Keays, Tubulins and brain development—The origins of functional specification, *Mol. Cell. Neurosci.* 84 (2017) 58–67.
- [76] J. Guo, C. Walss-Bass, R.F. Ludueña, The β isotypes of tubulin in neuronal differentiation, *Cytoskeleton* 67 (7) (2010) 431–441.
- [77] M. Mariani, R. Karki, M. Spennato, D. Pandya, S. He, M. Andreoli, et al., Class III β -tubulin in normal and cancer tissues, *Gene* 563 (2) (2015) 109–114.
- [78] M. Hafizi, A. Atashi, B. Bakhshandeh, M. Kabiri, S. Nadri, R.H. Hosseini, et al., MicroRNAs as markers for neurally committed CD133+/CD34+ stem cells derived from human umbilical cord blood, *Biochem. Genet.* 51 (3–4) (2013) 175–188.
- [79] B. Inang, A.E. Elcin, Y.M. Elcin, Human embryonic stem cell differentiation on tissue engineering scaffolds: effects of NGF and retinoic acid induction, *Tissue Eng. Part A* 14 (6) (2008) 955–964.
- [80] M.J. Robertson, P. Gip, D.V. Schaffer, Neural stem cell engineering: directed differentiation of adult and embryonic stem cells into neurons, *Front. Biosci.* 13 (1) (2008) 21–50.
- [81] R. Thompson, C. Casali, C. Chan, Forskolin and IBMX Induce Neural Transdifferentiation of MSCs Through Downregulation of the NRSF, *Sci. Rep.* 9 (1) (2019) 1–10.
- [82] S. Park, K.S. Lee, Y.J. Lee, H.A. Shin, H.Y. Cho, K.C. Wang, et al., Generation of dopaminergic neurons in vitro from human embryonic stem cells treated with neurotrophic factors, *Neurosci. Lett.* 359 (1–2) (2004) 99–103.
- [83] J.S. Meyer, M.L. Katz, J.A. Maruniak, M.D. Kirk, Neural differentiation of mouse embryonic stem cells in vitro and after transplantation into eyes of mutant mice with rapid retinal degeneration, *Brain Res.* 1014 (1–2) (2004) 131–144.
- [84] F. Scintu, C. Reali, R. Pillai, M. Badiali, M.A. Sanna, F. Argioli, et al., Differentiation of human bone marrow stem cells into cells with a neural phenotype: diverse effects of two specific treatments, *BMC Neurosci.* 7 (2006) 14.
- [85] K.J. Cho, K.A. Trzaska, S.J. Greco, J. McArdle, F.S. Wang, J.H. Ye, et al., Neurons derived from human mesenchymal stem cells show synaptic transmission and can be induced to produce the neurotransmitter substance P by interleukin-1 α , *Stem Cells.* 23 (3) (2005) 383–391.
- [86] I. Zwart, A.J. Hill, J. Girdlestone, M.F. Manca, R. Navarrete, C. Navarrete, et al., Analysis of neural potential of human umbilical cord blood-derived multipotent mesenchymal stem cells in response to a range of neurogenic stimuli, *J. Neurosci. Res.* 86 (9) (2008) 1902–1915.
- [87] T. Kondo, S.A. Johnson, M.C. Yoder, R. Romand, E. Hashino, Sonic hedgehog and retinoic acid synergistically promote sensory fate specification from bone marrow-derived pluripotent stem cells, *Proc. Natl. Acad. Sci. U S A.* 102 (13) (2005) 4789–4794.
- [88] L. Zhang, L.C. Seitz, A.M. Abramczyk, L. Liu, C. Chan, cAMP initiates early phase neuron-like morphology changes and late phase neural differentiation in mesenchymal stem cells, *Cell Mol. Life Sci.* 68 (5) (2011) 863–876.
- [89] M. Tio, K.H. Tan, W. Lee, T.T. Wang, G. Udolph, Roles of db-cAMP, IBMX and RA in aspects of neural differentiation of cord blood derived mesenchymal-like stem cells, *PLoS ONE* 5 (2) (2010) e9398.
- [90] A. Salimi, S. Nadri, M. Gholasi, K. Khajeh, M. Soleimani, Comparison of different protocols for neural differentiation of human induced pluripotent stem cells, *Mol. Biol. Rep.* 41 (3) (2014) 1713–1721.
- [91] A. Kotwal, Electrical stimulation alters protein adsorption and nerve cell interactions with electrically conducting biomaterials, *Biomaterials* 22 (10) (2001) 1055–1064.
- [92] N. Patel, M.M. Poo, Orientation of neurite growth by extracellular electric fields, *J. Neurosci.* 2 (4) (1982) 483–496.
- [93] G. Zhao, H. Qing, G. Huang, G.M. Genin, T.J. Lu, Z. Luo, et al., Reduced graphene oxide functionalized nanofibrous silk fibroin matrices for engineering excitable tissues, *NPG Asia Mater.* 10 (10) (2018) 982–994.
- [94] B. Guo, P.X. Ma, Conducting Polymers for Tissue Engineering, *Biomacromolecules* 19 (6) (2018) 1764–1782.
- [95] Schmidt CE, Shastri VR, Furnish EJ, Langer R, editors. *Electrical Stimulation Of Neurite Outgrowth And Nerve Regeneration. Proceedings of the 17th Southern Biomedical Engineering Conference; 1998 6-8 Feb. 1998.*
- [96] J.Y. Lee, C.A. Bashur, A.S. Goldstein, C.E. Schmidt, Polypyrrole-coated electrospun PLGA nanofibers for neural tissue applications, *Biomaterials* 30 (26) (2009) 4325–4335.
- [97] F. Pires, Q. Ferreira, C.A. Rodrigues, J. Morgado, F.C. Ferreira, Neural stem cell differentiation by electrical stimulation using a cross-linked PEDOT substrate: Expanding the use of biocompatible conjugated conductive polymers for neural tissue engineering, *Biochim. Biophys. Acta.* 1850 (6) (2015) 1158–1168.
- [98] L. Wang, Y. Wu, T. Hu, P.X. Ma, B. Guo, Aligned conductive core-shell biomimetic scaffolds based on nanofiber yarns/hydrogel for enhanced 3D neurite outgrowth alignment and elongation, *Acta Biomater.* 96 (2019) 175–187.
- [99] A. Rahmani, S. Nadri, H.S. Kazemi, Y. Mortazavi, M. Sojoodi, Conductive electrospun scaffolds with electrical stimulation for neural differentiation of conjunctiva mesenchymal stem cells, *Artif. Organs.* 43 (8) (2019) 780–790.
- [100] S. Wang, C. Sun, S. Guan, W. Li, J. Xu, D. Ge, et al., Chitosan/gelatin porous scaffolds assembled with conductive poly(3,4-ethylenedioxythiophene) nanoparticles for neural tissue engineering, *J. Mater. Chem. B.* 5 (24) (2017) 4774–4788.
- [101] N. Li, Q. Zhang, S. Gao, Q. Song, R. Huang, L. Wang, et al., Three-dimensional graphene foam as a biocompatible and conductive scaffold for neural stem cells, *Sci. Rep.* 3 (2013) 1604.